

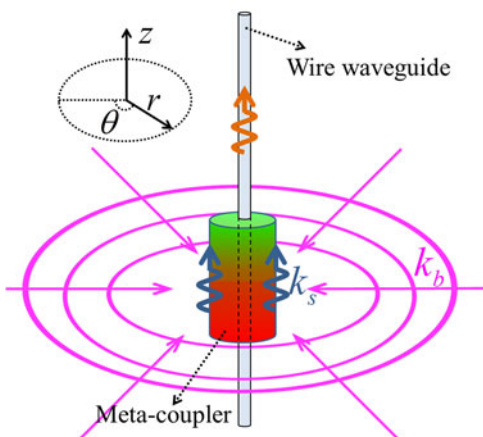
A Metacoupler for Converting Propagating Waves to Guided Waves in Wire Waveguides

Volume 9, Number 5, October 2017

Hongchen Chu

Jie Luo

Yun Lai



DOI: 10.1109/JPHOT.2017.2725299
1943-0655 © 2017 IEEE

A Metacoupler for Converting Propagating Waves to Guided Waves in Wire Waveguides

Hongchen Chu, Jie Luo, and Yun Lai

College of Physics, Optoelectronics and Energy & Collaborative Innovation Center of Suzhou Nano Science and Technology, Soochow University, Suzhou 215006, China

DOI:10.1109/JPHOT.2017.2725299

1943-0655 © 2017 IEEE. Translations and content mining are permitted for academic research only.
Personal use is also permitted, but republication/redistribution requires IEEE permission.
See http://www.ieee.org/publications_standards/publications/rights/index.html for more information.

Manuscript received June 7, 2017; revised July 6, 2017; accepted July 6, 2017. Date of publication July 13, 2017; date of current version July 28, 2017. This work is supported by the State Key Program for Basic Research of China (2014CB360505, 2012CB921501), National Natural Science Foundation of China (NSFC) (11374224), and Priority Academic Program Development of Jiangsu Higher Education Institutions (PAPD). Corresponding author: Yun Lai (e-mail: laiyun@suda.edu.cn).

Abstract: Propagating electromagnetic waves in free space cannot directly couple to guided waves in waveguides due to momentum mismatch. Here, we propose a method to design a metacoupler that can convert propagating waves into guided waves along wire waveguides in a noninvasive way. The metacoupler is attached to the wire waveguide and imposes an additional wave vector to the scattered waves, thus, filling the momentum gap between the propagating waves and guided waves. Numerical simulations have confirmed the conversion effect in corrugated metal wire and silicon wire waveguides.

Index Terms: Electromagnetic metamaterials, optical waveguides, surface waves.

1. Introduction

Recently, metasurfaces [1]–[21], as a unique type of planar metamaterial [22]–[25] consisting of designed electromagnetic units, have been proposed and shown to exhibit an unprecedented ability to manipulate the phase, polarization and amplitude of electromagnetic waves, leading to interesting phenomena like abnormal reflection and refraction [1]–[6], flat lens [7]–[9], cloaking [10]–[16], enhancement of holography and imaging [17], [18], and polarization control [19]–[21], etc. In particular, it has been theoretically and experimentally demonstrated that gradient metasurfaces are capable of converting propagating waves into surface waves (SWs) with nearly 100% efficiency [4], [5]. In the conversion process, an additional wave vector induced by gradient metasurfaces is imposed to the reflected or transmitted waves, which is beyond the wave number in the background medium [4]–[6]. As a result, the propagating waves are transformed into evanescent waves that propagate along the surface. Based on this concept, surface plasmon polariton (SPP) meta-couplers with high efficiency have been proposed [6].

However, the previous works on gradient metasurfaces as quasi-two-dimensional structures are mostly limited to incident plane waves. For quasi-one-dimensional wire waveguides and sensors, such as optical fiber and plasmonic nanowires [26], [27], new types of coupler are required. Very recently, gradient tip structures have been proposed to convert cylindrical propagating waves (CPWs) into guided waves (GWs) that propagate along a quasi-one-dimensional structure geometry [28]. However, the previous design requires the existence of a tip. This indicates that the geometry shape of waveguide has to be changed and the conversion process only happens at the end of the waveguide.

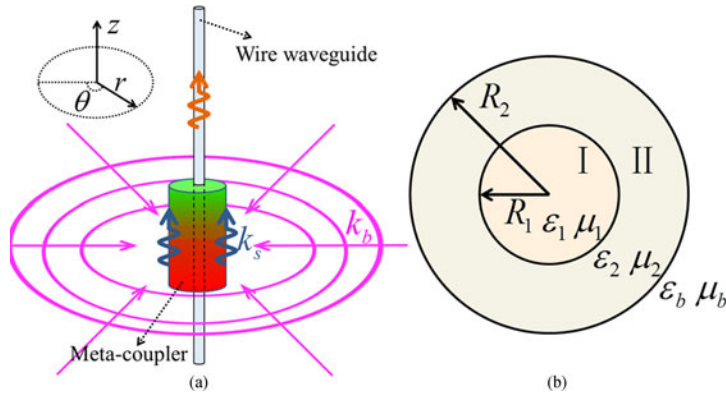


Fig. 1. (a) Schematic graph of a gradient meta-coupler that converts incident CPWs to GWs propagating upwards along a wire waveguide. (b) Top view of the model.

In this work, instead of designing tip structures, we design a type of meta-couplers to convert the propagating waves in free space to guided waves in wire waveguides in a noninvasive manner. The meta-coupler is simply attached to the waveguide and therefore the conversion process can happen in the middle part of the waveguide. The mechanism of such meta-couplers contains two steps. First, when CPWs are impinging onto the meta-coupler, the scattered waves will be adjusted to exhibit a linearly varying phase along the waveguide, i.e., an additional wave vector is imposed to the scattered waves. If the additional wave vector is larger than the wave number in the background medium, the scattered waves will turn into SWs propagating along the meta-coupler. Second, the SWs on the meta-coupler resonantly couple to waveguide modes in the wire waveguides when the momentum is matched. For demonstration, we have designed different meta-couplers for corrugated metal wire and silicon wire waveguides. The numerical results confirmed the conversion effect.

2. Descriptions of Model

The model we studied is composed of a gradient meta-coupler and a wire waveguide in the center, as illustrated in Fig. 1(a). Fig. 1(b) shows the top view of the model. The core (region I) and shell (region II) correspond to the wire waveguide and the meta-coupler, respectively, which are characterized by relative permittivity, relative permeability, radius of ε_1 , μ_1 , R_1 and ε_2 , μ_2 , R_2 , respectively. And the relative permittivity (permeability) of the background medium is ε_b (μ_b).

Now, we assume that the incident CPWs are of transverse electric (TE) polarization (with electric fields in the z direction). Then, the electric fields in the background medium can be expressed as,

$$\mathbf{E}_b = \sum_{n=-\infty}^{\infty} \left[a_n H_n^{(2)}(k_b r) e^{jn\theta} + b_n H_n^{(1)}(k_b r) e^{jn\theta} \right] \hat{z} \quad (1)$$

where $H_n^{(1)}$ and $H_n^{(2)}$ are the first and second kinds of n -th Hankel function. k_b are the wave number in the background medium. a_n and b_n are the coefficients corresponding to incident and scattered waves, respectively. Thus, the scattering coefficient is defined as $S_n = b_n/a_n$ for the core-shell model illustrated in Fig. 1(b). Taking the fields inside the core and shell, as well as the boundary conditions into consideration, the scattering coefficient S_n can be derived as [29],

$$S_n = \frac{b_n}{a_n} = \frac{\begin{vmatrix} H_n^{(2)}(k_2 r) + sH_n^{(1)}(k_2 r) & H_n^{(2)}(k_b r) \\ \sqrt{\frac{\varepsilon_2 \mu_b}{\varepsilon_b \mu_2}} [H_n^{(2)'}(k_2 r) + sH_n^{(1)'}(k_2 r)] & H_n^{(2)'}(k_b r) \end{vmatrix}}{\begin{vmatrix} H_n^{(2)}(k_2 r) + sH_n^{(1)}(k_2 r) & -H_n^{(1)}(k_b r) \\ \sqrt{\frac{\varepsilon_2 \mu_b}{\varepsilon_b \mu_2}} [H_n^{(2)'}(k_2 r) + sH_n^{(1)'}(k_2 r)] & -H_n^{(1)'}(k_b r) \end{vmatrix}} \quad (2)$$

with

$$S = \begin{vmatrix} J_n(k_1 r) & H_n^{(2)}(k_2 r) \\ \sqrt{\frac{\varepsilon_1 \mu_2}{\varepsilon_2 \mu_1}} J_n'(k_1 r) & H_n^{(2)'}(k_2 r) \end{vmatrix} / \begin{vmatrix} J_n(k_1 r) & -H_n^{(1)}(k_2 r) \\ \sqrt{\frac{\varepsilon_1 \mu_2}{\varepsilon_2 \mu_1}} J_n'(k_1 r) & -H_n^{(1)'}(k_2 r) \end{vmatrix}.$$

Here, J_n is the n -th Bessel function. k_1 (k_2) is the wave number in the core (shell). From the scattering coefficient S_n , the phase of the scattered waves φ can be obtained as $\varphi = \arg(S_n)$.

In the CPW-GW conversion process, the crucial functionality of the gradient meta-coupler is to generate scattered waves with a linearly varying phase along the meta-coupler. When there exists a phase difference of $\Delta\varphi$ within a distance of L in the z direction, an additional wave vector $k_a = \Delta\varphi/L$ along the z direction will be imposed on the scattered waves. Interestingly, if k_a is larger than the wave number in the background medium, i.e., $k_a > k_b$, the scattered waves will be evanescent in the radial direction in the background medium and be confined on the surface of the meta-coupler. Then, the driven SWs can resonantly couple to the eigenmodes in wire waveguides when the momentum is matched.

3. Metacoupler Design and Numerical Simulations

In the following, we consider two cases of corrugated metal wire and silicon wire waveguides. By designing appropriate meta-coupler, we numerically demonstrate the CPW-GW conversion effect.

In the first example, we design a meta-coupler for metal wire waveguides. It is known that metal wires can function as an efficient waveguide of surface plasmon polaritons (SPPs) in optical and terahertz frequency region [26], [27]. However, at low frequency region, the SPPs do not exist because the metals behave like perfect electric conductors (PECs), instead of plasmas with the negative permittivity. Interestingly, it has been demonstrated that periodically corrugated PEC structures can support SPP-like surface modes, i.e., the so-called spoof SPPs [30]–[34]. Here, we consider a PEC wire (radius $R_1 = 0.1\lambda$) with periodic subwavelength grooves. The period, depth and width of the grooves are $a = 0.19\lambda$, $d = 0.05\lambda$ and $w = 0.5a$, respectively. And λ is the wavelength in the background medium.

Before considering the linearly changing phase, we first study the scattering of a core-shell cylinder consisting of a PEC core and a dielectric shell. The background medium is free space. And we assume the angular momentum of the incident CPWs is zero. The outer radius of the dielectric shell is $R_2 = 0.2\lambda$. In Fig. 2(a), we plot the ε_2 -dependent phase φ of the scattered waves, showing that φ covers the range from $-\pi$ to $-\pi$ as ε_2 increases from 1 to 51.68.

Then, we consider a meta-coupler composed of a shell with a gradient ε_2 that varies along the axis (i.e., ε_2 is the function of z). The meta-coupler has a length of L in the z direction. Due to the gradient ε_2 , the phase of the scattered waves also varies along the axis. According to the requirement of conversion, the phase should vary linearly as a function of z , and the phase difference $\Delta\varphi$ within the distance of L should satisfy $\Delta\varphi/L > k_b$. As an example, in Fig. 2(b), we present one possible distribution of the phase that fulfills the above requirements. Combined with Fig. 2(a), we can find out the required distribution of ε_2 , as shown in Fig. 2(c).

To verify the CPW-GW conversion, numerical simulations are performed by employing the finite-element software COMSOL Multiphysics. In this numerical simulation, the incident CPW is excited by given a background electric field $E_b = H_0^{(2)}(k_b r)$. The length of the meta-coupler is set to $L = 0.95\lambda$, and the ε_2 -distribution of the meta-coupler as shown in Fig. 2(c) is set by utilizing the interpolation function in COMSOL. Perfect matched layers have been set around the region to absorb the scattered waves. The snapshots of radial component of the electric fields E_r are shown in Fig. 2(d). Since the incident waves do not have electric field component E_r , the existence of E_r is purely induced by GWs propagating along the axis. It is seen that the GWs are well confined on the corrugated PEC wire and exponentially decay in the radial direction in free space. Furthermore, we can see that the GWs propagate upwards because the addition wave vector generated by the meta-coupled is in the upward direction. The CPW-GW conversion is confirmed.

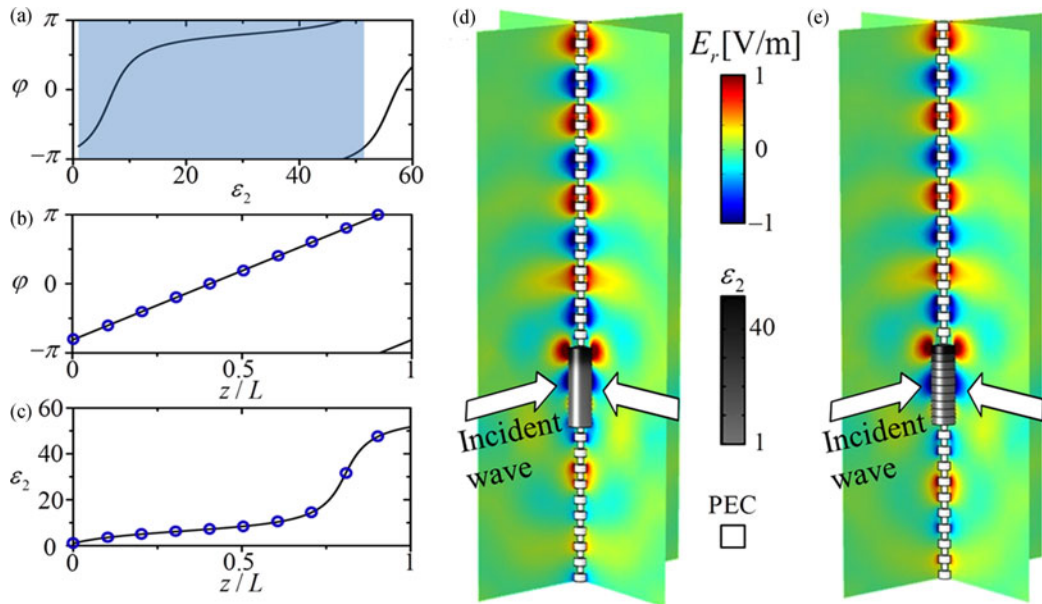


Fig. 2. (a) Phase of the scattered waves as the function of ε_2 . (b) The desired linearly varying phase. (c) Required distribution of ε_2 along the meta-coupler. Snapshots of the radial component of electric fields E_r , by using a (d) gradient, (e) discretized meta-coupler. The wire waveguide is a periodically corrugated PEC wire.

In practice, it is difficult to realize the continuously varying ε_2 . Therefore, in Fig. 2(e), a discretized meta-coupler with 10 segments is used. These segments have constant ε_2 of 1, 3.54, 4.99, 6.10, 7.15, 8.37, 10.18, 14.01, 29.10 and 47.19 separately, which are denoted by blue circles in Fig. 2(c). And the corresponding phase is shown by blue circles in Fig. 2(b). In Fig. 2(e), the CPW-GW conversion effect is also confirmed.

Moreover, we have calculated conversion efficiency, which is defined by $\eta = P_S/P_0$, where P_0 is the time-averaged power flow of the incident CPWs impinging onto the coupler and P_S is the power flow carried by the GWs. Here, P_S is calculated by the integration $P_S = \iiint_S \mathbf{P} d\mathbf{S}$, where \mathbf{P} is the time-averaged Poynting vector, and \mathbf{S} is a circular plate (with a radius of 0.8λ) in $r\theta$ -plane at a distance of λ to the top of the meta-coupler. According to the simulation results in Fig. 2(e), the conversion efficiency is found to be 38%.

The loss of the efficiency can be understood from the insights of two conversion steps. First, the CPWs are converted to GWs on the meta-coupler, which has been demonstrated to be highly efficient [28]. Second, the GWs on the surface of the meta-coupler couple to the wire waveguide modes. Due to the sudden change of radius and discontinuity of parameters, the conversion efficiency in this step is relatively low. To mitigate this problem, one way is to make the meta-coupler as thin as possible. However, in order to meet the requirement of 2π phase change, the decrease of the thickness of the meta-coupler would also lead to the increase of the required permittivity, which may lead to loss and other complicated issues in practical applications.

The proposed quasi-one-dimensional meta-couplers inherit the advantages of gradient metasurface coupler [4] linking propagating plane waves and surface waves. For example, compared to conventional prism coupler, the thickness of the meta-coupler is sub-wavelength (i.e., 0.1λ), which means that it is of small size and light weight. On the other hand, although gratings as another type of propagating waves to SWs coupler have sub-wavelength thickness, under normal incidence it always generates two types of SWs with opposite wave vector due to the geometric symmetry, while the proposed meta-coupler under the same normal illumination generates SWs with the desired wave vector only. In addition, the conversion efficiency of the meta-coupler is quite higher than that of traditional prism and grating couplers without any special optimization [6].

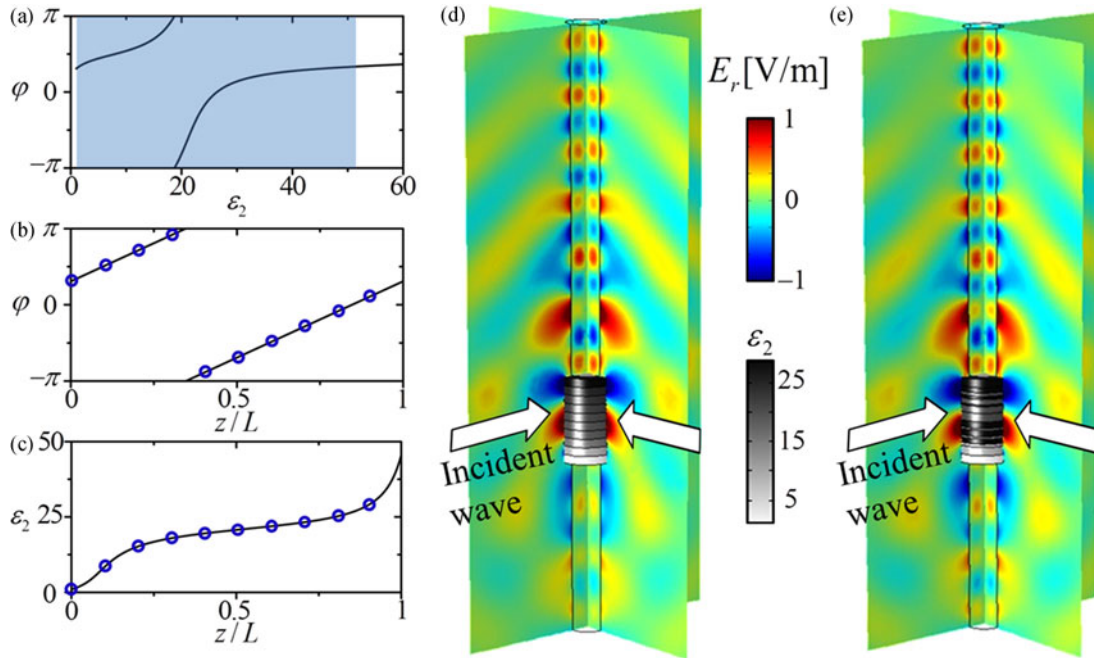


Fig. 3. (a) Phase of the scattered waves as the function of ε_2 . (b) The desired linearly varying phase. (c) Required distribution of ε_2 along the meta-coupler. (d) Snapshots of the radial component of electric fields E_r by using a discretized meta-coupler. (e) The meta-coupler in (d) is replaced by subwavelength multilayers consisting of four different dielectric materials. The wire waveguide is a silicon wire.

In the second example, we utilize a meta-coupler to convert the CPWs into GWs in a silicon wire waveguide which is one of the most common photonics devices. The radii of the silicon wire ($\varepsilon_1 = 11.7$) and the meta-coupler are $R_1 = 0.2\lambda$ and $R_2 = 0.3\lambda$, respectively. The background medium is free space. Similarly, we first study the phase φ of the scattered waves by a uniform dielectric shell with a silicon core. The ε_2 -dependent φ is plotted in Fig. 3(a), showing that φ covers the full phase range of 2π as the increase of ε_2 . Then, we consider the gradient meta-coupler. In Fig. 3(c), we present the required ε_2 -distribution to obtain the linearly varying phase in Fig. 3(b). In numerical verification, the ε_2 of the meta-coupler is discretized into 10 layers, as indicated by the blue circles in Fig. 3(c), which produce the discretized phases shown by the blue circles in Fig. 3(b). The E_r -distribution in Fig. 3(d) demonstrates that the CPWs in air are indeed converted to GWs propagating upwards along the silicon wire waveguide. According to the simulation results in Fig. 2(e), the conversion efficiency is found to be 25%.

Moreover, the design of ten segments can be further simplified by using fewer materials. Here, four dielectric materials with relative permittivities of 1, 8.4, 20.7 or 28.9 are utilized to realize the required discretized ε_2 . In Fig. 3(e), each segment is composed of two dielectric layers, whose effective relative permittivity is described by Maxwell-Garnett theory [28], [35]. The distribution of E_r in Fig. 3(e) also demonstrates the CPW-GW conversion. And the calculated conversion efficiency is 21%.

In the above models, materials with relatively high refractive index are required, which can be readily obtained in the microwave frequency regime by using materials like ceramic. In addition, artificial dielectrics with high refractive index has been constructed by using metallic gratings with periodic slits [36]–[38] and metamaterials composed of sub-wavelength resonators [39], [40]. We note that in the CPW-GW conversion progress, the linearly varying reflection phase shifts and the additional wave vector imposed on the scattering waves rather than the gradient relative permittivity is vital. So, to get the linearly varying reflection phase, many other methods except for introducing gradient relative permittivity can be utilized, such as by introducing gradient relative permeability, assembling arrays of scatterers generating gradient scattering phase, and adopting homogeneous

media with gradient geometric parameters. These methods can mitigate the requirement of high-index media.

4. Discussions and Conclusion

The concept of the proposed meta-coupler and the principle of CPWs-GWs conversion could be important for coupling propagating waves to on-chip waveguides. Normally, light is coupled to chip wire waveguides via fiber or grating structures [41], [42]. Our work provides an efficient and flexible method to couple propagating waves into on-chip waveguides via sub-wavelength meta-couplers. Although the demonstration in this work is of circular cross section, the principle is general and can be extended to wire waveguide with other cross-sectional shapes.

In summary, we have proposed a method to convert CPWs to GWs by using a gradient meta-coupler. The gradient meta-coupler can generate linearly varying phase, and thus imposes an additional wave vector to scattered waves. When the additional wave vector is larger than the wave number in the background medium, scattered waves will be confined on the surface of the meta-coupler, and thus couple to the GWs in the wire waveguides. As demonstrations, we have designed meta-couplers for corrugated PEC wire and silicon wire waveguides. Unlike previous approaches of using gradient tips, such a method is noninvasive to the wire waveguides.

Acknowledgment

The authors would like to thank the anonymous reviewers for their valuable suggestions.

References

- [1] N. Yu *et al.*, "Light propagation with phase discontinuities: Generalized laws of reflection and refraction," *Science*, vol. 334, no. 6054, pp. 333–337, Oct. 2011.
- [2] X. Ni, N. K. Emani, A. V. Kildishev, A. Boltasseva, and V. M. Shalaev, "Broadband light bending with plasmonic nanoantennas," *Science*, vol. 335, no. 6067, Jan. 2012, Art. no. 427.
- [3] C. Pfeiffer and A. Grbic, "Metamaterial Huygens' surfaces: Tailoring wave fronts with reflectionless sheets," *Phys. Rev. Lett.*, vol. 110, no. 19, May. 2013, Art. no. 197401.
- [4] S. Sun, Q. He, S. Xiao, Q. Xu, X. Li, and L. Zhou, "Gradient-index meta-surfaces as a bridge linking propagating waves and surface waves," *Nat. Mater.*, vol. 11, no. 5, pp. 426–431, Apr. 2012.
- [5] S. Sun *et al.*, "High-efficiency broadband anomalous reflection by gradient meta-surfaces," *Nano Lett.*, vol. 12, no. 12, pp. 6223–6229, Nov. 2012.
- [6] W. Sun, Q. He, S. Sun, and L. Zhou, "High-efficiency surface plasmon meta-couplers: Concept and microwave-regime realizations," *Light, Sci. Appl.*, vol. 5, no. 1, Jan. 2016, Art. no. e16003.
- [7] F. Aieta *et al.*, "Aberration-free ultrathin flat lenses and axicons at telecom wavelengths based on plasmonic metasurfaces," *Nano Lett.*, vol. 12, no. 9, pp. 4932–4936, Sep. 2012.
- [8] F. Aieta, M. A. Kats, P. Genevet, and F. Capasso, "Multiwavelength achromatic metasurfaces by dispersive phase compensation," *Science*, vol. 347, no. 6228, pp. 1342–1345, Mar. 2015.
- [9] M. Khorasaninejad, W. T. Chen, R. C. Devlin, J. Oh, A. Y. Zhu, and F. Capasso, "Metалenses at visible wavelengths: Diffraction-limited focusing and subwavelength resolution imaging," *Science*, vol. 352, no. 6290, pp. 1190–1194, Jun. 2016.
- [10] A. Alù, "Mantle cloak: Invisibility induced by a surface," *Phys. Rev. B*, vol. 80, no. 24, Dec. 2009, Art. no. 245115.
- [11] P. Chen, C. Argyropoulos, and A. Alù, "Broadening the cloaking bandwidth with non-foster metasurfaces," *Phys. Rev. Lett.*, vol. 111, no. 23, Dec. 2013, Art. no. 233001.
- [12] F. Monticone and A. Alù, "Do cloaked objects really scatter less?" *Phys. Rev. X*, vol. 3, no. 4, Oct. 2013, Art. no. 41005.
- [13] J. Zhang, Z. Lei Mei, W. Ru Zhang, F. Yang, and T. Jun Cui, "An ultrathin directional carpet cloak based on generalized Snell's law," *Appl. Phys. Lett.*, vol. 103, no. 15, Oct. 2013, Art. no. 151115.
- [14] X. Ni, Z. J. Wong, M. Mrejen, Y. Wang, and X. Zhang, "An ultrathin invisibility skin cloak for visible light," *Science*, vol. 349, no. 6254, pp. 1310–1314, Sep. 2015.
- [15] Y. Yang *et al.*, "Full-polarization 3D metasurface cloak with preserved amplitude and phase," *Adv. Mater.*, vol. 28, no. 32, pp. 6866–6871, May. 2016.
- [16] D. L. Sounas, R. Fleury, and A. Alù, "Unidirectional cloaking based on metasurfaces with balanced loss and gain," *Phys. Rev. Appl.*, vol. 4, no. 1, Jul. 2015, Art. no. 14005.
- [17] X. Ni, A. V. Kildishev, and V. M. Shalaev, "Metasurface holograms for visible light," *Nat. Commun.*, vol. 4, Nov. 2013, Art. no. 2807.
- [18] L. Huang *et al.*, "Three-dimensional optical holography using a plasmonic metasurface," *Nat. Commun.*, vol. 4, Nov. 2013, Art. no. 2808.

- [19] N. K. Grady *et al.*, "Terahertz metamaterials for linear polarization conversion and anomalous refraction," *Science*, vol. 340, no. 6138, pp. 1304–1307, Jun. 2013.
- [20] S. Jiang *et al.*, "Controlling the polarization state of light with a dispersion-free metastructure," *Phys. Rev. X*, vol. 4, no. 2, May. 2014, Art. no. 21026.
- [21] S. L. Jia, X. Wan, D. Bao, Y. J. Zhao, and T. J. Cui, "Independent controls of orthogonally polarized transmitted waves using a huygens metasurface," *Laser Photon. Rev.*, vol. 9, no. 5, pp. 545–553, Aug. 2015.
- [22] J. B. Pendry, A. J. Holden, W. J. Stewart, and I. I. Youngs, "Extremely low frequency plasmons in metallic mesostructures," *Phys. Rev. Lett.*, vol. 76, no. 25, pp. 4773–4776, Jun. 1996.
- [23] J. B. Pendry, A. J. Holden, D. J. Robbins, and W. J. Stewart, "Magnetism from conductors and enhanced nonlinear phenomena," *IEEE Trans. Microw. Theory Techn.*, vol. 47, no. 11, pp. 2075–2084, Nov. 1999.
- [24] D. R. Smith, W. J. Padilla, D. C. Vier, S. C. Nemat-Nasser, and S. Schultz, "Composite medium with simultaneously negative permeability and permittivity," *Phys. Rev. Lett.*, vol. 84, no. 18, pp. 4184–4187, May. 2000.
- [25] R. A. Shelby, D. R. Smith, and S. Schultz, "Experimental verification of a negative index of refraction," *Science*, vol. 292, no. 5514, pp. 77–79, Apr. 2001.
- [26] K. Wang and D. M. Mittleman, "Metal wires for terahertz wave guiding," *Nature*, vol. 432, no. 7015, pp. 376–379, Nov. 2004.
- [27] K. Wang and D. M. Mittleman, "Dispersion of surface plasmon polaritons on metal wires in the terahertz frequency range," *Phys. Rev. Lett.*, vol. 96, no. 15, Apr. 2006, Art. no. 157401.
- [28] H. C. Chu, J. Luo, and Y. Lai, "Efficient way to convert propagating waves into guided waves via gradient wire structures," *Opt. Lett.*, vol. 41, no. 15, Aug. 2016, Art. no. 3551.
- [29] P. Bai, Y. Wu, and Y. Lai, "Multi-channel coherent perfect absorbers," *Europhys. Lett.*, vol. 114, no. 2, May. 2016, Art. no. 28003.
- [30] J. B. Pendry, L. Martín-Moreno, and F. J. García-Vidal, "Mimicking surface plasmons with structured surfaces," *Science*, vol. 305, no. 5685, pp. 847–848, Aug. 2004.
- [31] F. J. García-Vidal, L. Martín-Moreno, and J. B. Pendry, "Surfaces with holes in them: new plasmonic metamaterials," *J. Opt. A*, vol. 7, no. 2, pp. S97–S101, Jan. 2005.
- [32] S. A. Maier, S. R. Andrews, L. Martín-Moreno, and F. J. García-Vidal, "Terahertz surface plasmon-polariton propagation and focusing on periodically corrugated metal wires," *Phys. Rev. Lett.*, vol. 97, no. 17, Oct. 2006, Art. no. 176805.
- [33] X. Shen and T. J. Cui, "Ultrathin plasmonic metamaterial for spoof localized surface plasmons," *Laser Photon. Rev.*, vol. 8, no. 1, pp. 137–145, Nov. 2014.
- [34] H. F. Ma, X. Shen, Q. Cheng, W. X. Jiang, and T. J. Cui, "Broadband and high-efficiency conversion from guided waves to spoof surface plasmon polaritons," *Laser Photon. Rev.*, vol. 8, no. 1, pp. 146–151, Nov. 2014.
- [35] J. C. Maxwell Garnett, "Colours in metal glasses and in metallic films," *Philosophical Trans. Royal Soc. A, Math., Phys. Eng. Sci.*, vol. 203, no. 359–371, pp. 385–420, Jun. 1904.
- [36] J. T. Shen, P. B. Catrysse, and S. Fan, "Mechanism for designing metallic metamaterials with a high index of refraction," *Phys. Rev. Lett.*, vol. 94, no. 19, May. 2005, Art. no. 197401.
- [37] A. Pimenov and A. Loidl, "Experimental demonstration of artificial dielectrics with a high index of refraction," *Phys. Rev. B*, vol. 74, no. 19, Nov. 2006, Art. no. 193102.
- [38] M. Naserpour, C. J. Zapata-Rodríguez, C. Diaz-Avino, M. Hashemi, and J. J. Miret, "Ultrathin high-index metasurfaces for shaping focused beams," *Appl. Opt.*, vol. 54, no. 25, pp. 7586–7591, Sep. 2015.
- [39] Z. Liu *et al.*, "Polarization-independent metamaterial with broad ultrahigh refractive index in terahertz region," *Opt. Mater. Exp.*, vol. 5, no. 9, Sep. 2015, Art. no. 1949.
- [40] S. Tan *et al.*, "Terahertz metasurfaces with a high refractive index enhanced by the strong nearest neighbor coupling," *Opt. Exp.*, vol. 23, no. 22, p. 29222, Nov. 2015.
- [41] L. H. Gabrielli, D. Liu, S. G. Johnson, and M. Lipson, "On-chip transformation optics for multimode waveguide bends," *Nat. Commun.*, vol. 3, no. 1217, Nov. 2012, Art. no. 1217.
- [42] H. Jin *et al.*, "On-chip generation and manipulation of entangled photons based on reconfigurable lithium-niobate waveguide circuits," *Phys. Rev. Lett.*, vol. 113, Sep. 2014, Art. no. 103601.